

PCCP

Accepted Manuscript



This is an *Accepted Manuscript*, which has been through the Royal Society of Chemistry peer review process and has been accepted for publication.

Accepted Manuscripts are published online shortly after acceptance, before technical editing, formatting and proof reading. Using this free service, authors can make their results available to the community, in citable form, before we publish the edited article. We will replace this *Accepted Manuscript* with the edited and formatted *Advance Article* as soon as it is available.

You can find more information about *Accepted Manuscripts* in the [Information for Authors](#).

Please note that technical editing may introduce minor changes to the text and/or graphics, which may alter content. The journal's standard [Terms & Conditions](#) and the [Ethical guidelines](#) still apply. In no event shall the Royal Society of Chemistry be held responsible for any errors or omissions in this *Accepted Manuscript* or any consequences arising from the use of any information it contains.

Cite this: DOI: 10.1039/c0xx00000x

www.rsc.org/xxxxxx

ARTICLE TYPE

Connecting supramolecular bond lifetime and network mobility for scratch healing in poly(butyl acrylate) ionomers containing sodium, zinc and cobalt

Ranjita K. Bose,^a Nico Hohlbein,^b Santiago J. Garcia,^{a,*} Annette M. Schmidt,^{b,†} Sybrand van der Zwaag^a⁵ Received (in XXX, XXX) Xth XXXXXXXXX 20XX, Accepted Xth XXXXXXXXX 20XX

DOI: 10.1039/b000000x

In this work, we correlate network dynamics, supramolecular reversibility and the macroscopic surface scratch healing behavior for a series of elastomeric ionomers based on an amorphous backbone with varying fractions of carboxylate pendant groups completely neutralized by Na⁺, Zn²⁺ or Co²⁺ as the counter ions. Our results based on temperature dependent dynamic rheology with simultaneous FTIR analysis clearly indicate that the effective supramolecular bond lifetime (τ_b) is an important parameter to ascertain the ideal range of viscoelasticity for good macroscopic healing. The reversible coordination increased with higher valence metal ions and ionic content. Both rheological and spectroscopic analyses show a decrease in supramolecular assembly with temperature. The temperature dependent τ_b was used to calculate the activation energy (E_a) of dissociation for the ionic clusters. According to self-healing experiments based on macroscale surface scratching, a supramolecular bond lifetime between 10 and 100 s results in samples with complete surface scratch healing and good mechanical robustness.

Introduction

Self-healing in polymeric systems can be broadly classified into extrinsic and intrinsic healing approaches.¹⁻³ While in extrinsically healing systems, the healing agent is added to the matrix material as micro- or nanocapsules or fibres,⁴ intrinsic systems rely on the natural chemical or physical reversibility of the material. This reversibility can be in the form of covalent bonds,⁵⁻¹⁰ metal-ligand interactions,¹¹⁻¹³ hydrogen bonds,¹⁴⁻¹⁶ or ionic supramolecular clusters,^{17, 18} to name a few. The advantage of the intrinsic self-healing approach based on dynamic self-assembly in polymeric materials is that the high density of intermolecular interactions can ultimately result in mechanically robust materials under working conditions, while upon damage, the molecular rearrangement induces repair of the damaged site. In addition, by tuning the nature, strength and concentration of the dynamic bond the supramolecular networks become sensitive to environmental variables, such as temperature, allowing design and synthesis of tunable or responsive reversible polymer networks.

The two key parameters for the design of self-healing supramolecular polymers are chain dynamics and strength of reversible interactions. The dynamic nature of the defining interactions determines the mechanical properties of a material and the time scale of reversibility, which is referred to as the supramolecular bond lifetime (τ_b). τ_b has recently shown to be a key characteristic describing the dynamic nature of supramolecular interactions.¹⁹⁻²³ When the bond lifetime is short, the macromolecular assembly is amenable to flow, whereas a

long lifetime yields materials without dynamic behavior. It has been reported that in an intermediate range of bond lifetimes, $1 \mu\text{s} < \tau_b < 1 \text{ min}$, materials with attractive and tunable properties such as adaptability, responsiveness and self-healing can be obtained.²⁴

In the field of supramolecular self-healing polymers, ionomers are one of the most studied systems due to their high versatility.^{17, 18, 25, 26} Ionomers are polymers with a nonpolar backbone and up to 15 mol% of pendant ionic groups. The development of intermolecular interactions and reversible crosslinks in these materials is due to microphase separation into a polar, cluster-forming ionic phase, and the non-polar polymer phase. In these networks, the thermally reversible crosslinks are formed by the interaction of the metal ion with the carboxylate group, which give rise to multiplets and clusters of these reversible bonds as shown schematically in Figure 1. Therefore the effective supramolecular bond lifetime (τ_b) in ionomers corresponds to the relaxation time of these reversible tie points. τ_b depends on temperature, fraction of ion content and molecular weight of the polymers. Apart from τ_b , the parameters associated with the strength of a supramolecular network are the average molecular weight between physical and chemical crosslinks (segment length M_c) and the strength of the reversible interactions.^{21, 27-30} The relation between the network strength and the extent of reversible interactions determine the mechanical properties of the polymer and its healing efficiency. The corresponding time-dependent dynamic mechanical properties can be measured by frequency-modulated rheological measurements.

The present work is a first detailed systematic study on the role of the ionic fraction and type of metal counter-ion for the temperature-dependent dynamic-mechanical properties of

ionomeric elastomers, and their correlation to the macroscopic surface scratch healing efficiency. Model copolymers of butyl acrylate with varying molar fraction of acrylic acid units, yet with constant molecular weight were synthesized, and subsequently neutralized with different metal salts of sodium, zinc and cobalt were used. Sodium and zinc are some of the most commonly studied metal ions in ionomers,³¹⁻³³ and thus used in this work to study the differences between monovalent and divalent cations. Cobalt was also used to further compare the differences between different divalent transition metal cations. Microscale scratching followed by controlled annealing was used to quantify the healing characteristics.

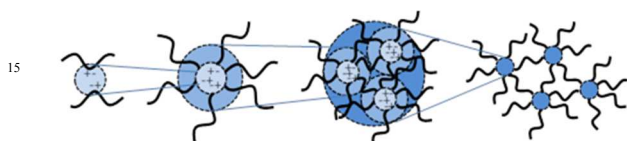


Fig 1. Schematic representation of the hierarchical formation of the ionomer morphology: ion pair \rightarrow multiplet \rightarrow ionic cluster \rightarrow network with encircled regions of restricted polymer mobility.

Experimental

Materials

n-Butylacrylate (nBA) (Aldrich, 99%) and *tert*-butylacrylate (tBA) (Aldrich 98%) were purified by filtering over a basic aluminium oxide plug and flushing with argon (Linde) for 20 min. Methyl-2-bromopropionate (MBrP) (Aldrich, 97%) was used without further purification. CuBr (Aldrich, 98%) was purified by stirring with concentrated acetic acid for 12 h, filtered, washed with ethanol and diethylether, and dried under vacuum at 75 °C. *N,N,N',N'',N'''*-pentamethyl diethylene triamine (PMDETA) (Aldrich, 99%) was used without further purification. Trifluoroacetic acid (Solvay Organics, 99%) was used for hydrolyzation. The corresponding amount of zinc(II)acetate dihydrate (Merck, 99.5%), cobalt(II)acetate tetrahydrate (Merck, 99%) or sodium hydroxide (Fisher Chemicals, >97%) dissolved in 1,3-dioxane (Applchem, 99%) was used for the synthesis of the ionomers.

Polymer Synthesis

Ionomers with a controlled ion fraction and molar mass were prepared by a three-step procedure according to a recently published protocol.³⁴ First, copolymers of *n*-butylacrylate and *tert*-butylacrylate were obtained by atom-transfer radical polymerization (ATRP) with CuBr/PMDETA, with a molar fraction of *tert*-butylacrylate, later resulting in ionic groups, between 2 to 10 mol%. After polymer workup, the pendant *tert*-butyl groups were quantitatively hydrolyzed to carboxylic acid moieties with trifluoroacetic acid. Neutralization of the carboxylic acid groups to carboxylates of various metal cations was performed in 1,3-dioxane at 80 °C for 2 h by addition of the respective metal acetate (Zn^{2+} , Co^{2+}) or hydroxide (Na^+). The ionomers are labelled with *PM*-*x*; with *M*: metal counter ion, *x*: molar percentage of ionized repeating units. All synthesized polymers were characterized by NMR and GPC and details are presented elsewhere.³⁴

Differential scanning calorimetry (DSC)

Differential calorimetric thermal analysis to obtain the glass transition temperature (T_g) and the ionic cluster transition temperature (T_i) were performed via DSC using a heat-flux calorimeter DSC-1 (Mettler-Toledo), and measured from -100 °C to 150 °C with a heating rate of 10 K min⁻¹.

Rheology with in situ FTIR

Rheological experiments with *in situ* Fourier transform infrared (FTIR) spectroscopy were performed on a combined system (Haake Mars III, Thermofisher coupled with Nicolet iS10) with integrated data collection. The bottom plate of the rheometer has the diamond attenuated total reflectance (ATR) element which allows for *in situ* spectroscopic measurements while simultaneously measuring viscoelastic changes. Oscillatory shear rheology with 20 mm diameter stainless steel parallel plate geometry was used for all the experiments. For all the samples, thickness was between 1-2 mm, and a constant shear strain γ of 1%, which was within the linear viscoelastic regime of the materials, was used. Frequency sweep experiments between 10² Hz - 10⁻³ Hz were performed at temperatures of 25, 40, 60, and 80 °C, and with an isothermal hold for 20 min prior to each temperature step. FTIR data was collected immediately after every frequency sweep measurement. Quantitative information for cluster formation was obtained from FTIR by monitoring the carboxylic acid coordination peak.³⁵ The peak area of the carboxylic coordination peak ranging from 1660 cm⁻¹ -1512 cm⁻¹ was normalized to the peak area of the main carbonyl stretch ranging from 1776-1667 cm⁻¹ and centered at 1721 cm⁻¹.

Table 1. Theoretical and experimental polymer composition and nomenclature.

Theoretical polymer	Experimental ion Nomenclature content (%)	
P(nBA-2.0-co-AAM)-2.0%	2.0	PM-2
P(nBA-3.0-co-AAM)-3.0%	2.6	PM-3
P(nBA-4.0-co-AAM)-4.0%	4.2	PM-4
P(nBA-5.0-co-AAM)-5.0%	5.2	PM-5
P(nBA-6.0-co-AAM)-6.0%	6.2	PM-6
P(nBA-8.0-co-AAM)-8.0%	8.6	PM-8
P(nBA-9.0-co-AAM)-9.0%	9.2	PM-9
P(nBA-10.0-co-AAM)-10.0%	9.9	PM-10

where M indicates the metal ion Na^+ , Zn^{2+} or Co^{2+} .

Scratch testing and macroscopic healing

Micro-scratch testing (CSM micro-scratch tester) was performed to obtain quantitative damage healing data following a variant of a previously described protocol.³⁶ Samples were melt-pressed onto aluminum substrates and were kept for at least 24 h at room temperature to equilibrate. Using a 100 μm diameter Rockwell diamond tip, first a pre-scan at 0.03 N load was performed to gauge the profile of each coating and subtract the coating inhomogeneity from the scratch depth measurements. Trial scratches were produced using a progressive load from 0.03 to 30 N along a 10 mm length to determine the critical load at which the tip of the indenter touched the aluminum substrate. Constant load scratches of 10 mm length were subsequently performed at load values just above the measured critical loads, typically between 0.5 and 2 N. Scratches were performed at 25 °C, which

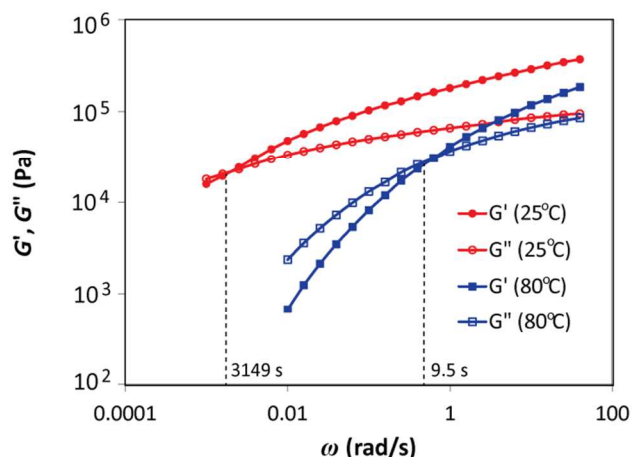


Fig 2. Storage modulus (G') and loss modulus (G'') of ionomer PCo-3 at 25 °C and 80 °C as a function of frequency.

is well above the T_g of the polymers and below their ionic cluster transition temperatures (T_i). A post-scan with 0.03 N load along the same track as the original scratch was performed within 60 seconds after the completion of the high constant load scan to determine and quantify the elastic recovery. The effective scratch depth (S_0) was obtained by subtracting the elastic recovery from the penetration depth. After determination of S_0 , each sample was either kept at 25 °C for up to 24 hours or heated on the heating stage incorporated in the scratch tester at a rate of 50 °C min^{-1} and isothermally held at 50 °C or 100 °C up to 24h; this process being the healing step. The depth of the scratch was monitored every 10 min by applying a minimal load of 0.03 N on the same scratch, allowing determination of the scratch healing kinetics. The self-healing efficiency was calculated using equation (1) $\eta = (1 - S_t/S_0) \cdot 100$ (1) where S_t is the scratch depth measured at healing time t .

Results and discussion

Polymer synthesis and characterisation

All ionomers had a molar mass in the range of $M_w \sim 42,000 \text{ g}\cdot\text{mol}^{-1}$ with a low polydispersity index (PDI ~ 1.1), as verified by GPC. The theoretical and experimental ion fraction for each ionomer and the nomenclature used in this work is shown in Table 1. The glass transition temperature T_g is below -30 °C for all the ionomers, indicating an excellent flexibility of the polymer main chain under ambient conditions. The characteristic transition temperature of the ionic clusters, T_i , is around +50 °C for ionomers with an ionic fraction below 6 mol%, and increases up to 170 °C for increasing ionomer content. The observed trend is similar for the three series of ionomers with different counter ions.

All ionomers of the three metal ion series under investigation show the typical frequency sweep spectrum of dynamic supramolecular networks as reported elsewhere.³⁷ As can be seen in the sample spectrum of PCo-3 (Figure 2), at room temperature the storage/elastic modulus G' is larger than the loss/viscous modulus G'' and the supramolecular bonds remain intact and effectively prevent molecular slippage under high frequency deformation. However, at the long time scales (low frequency range), G' is lower than G'' indicating the supramolecular bonds

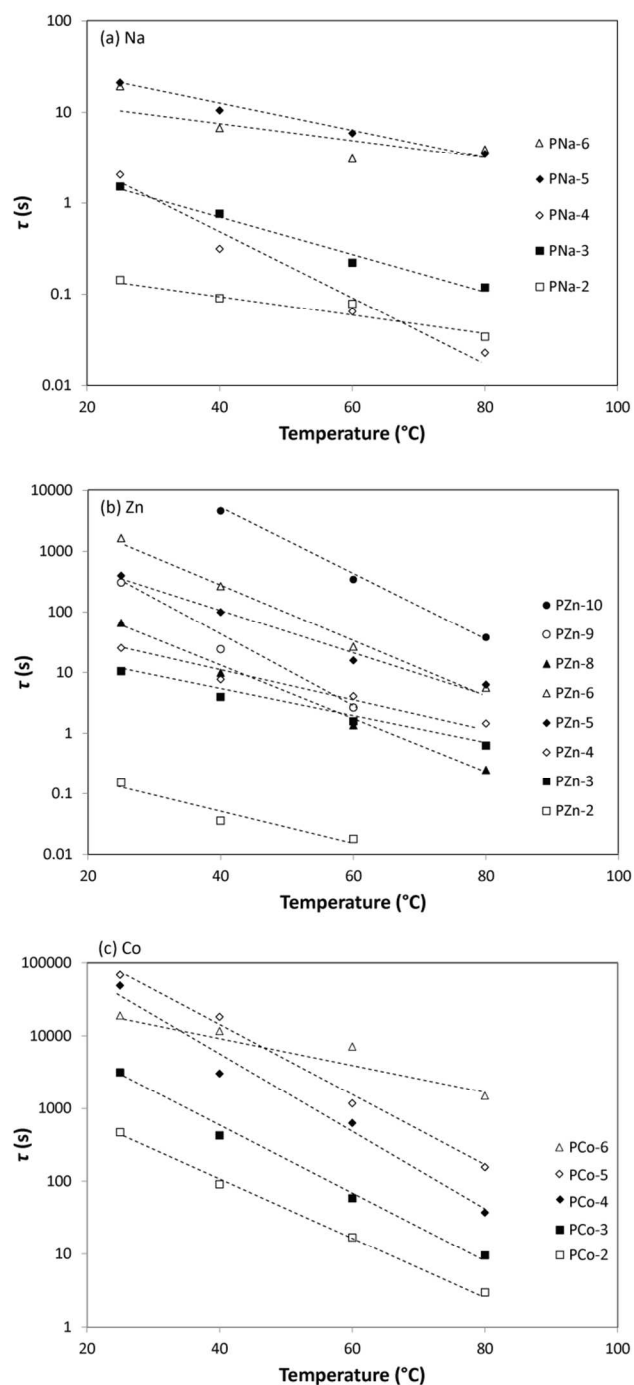


Fig 3. Supramolecular bond lifetime (τ_b) as a function of temperature for (a) PNa, (b) PZn, (c) PCo series. Dotted lines are a guide to the eye.

are subjected to a rearrangement during the slow perturbation. These phenomena appear more evident at temperatures above the ionic transition temperature as seen in Figure 2 at 80 °C. The transition between the time domains dominated by the elastic and the viscous behavior is given by the crossover frequency (ω_{cr}) of the G' and G'' curves, time $\tau_b = 2\pi/\omega_{cr}$ is good measure of the ionic relaxation timescale, henceforth referred to as the supramolecular bond lifetime (τ_b). This parameter is the characteristic time scale for the dissociation and association of

the dynamic bonds responsible for the network mobility is thus crucial for a proper understanding of the dynamic behavior of the material.³⁸

τ_b as a function of temperature is shown in Figure 3 for the (a) PNa, (b) PZn and (c) PCo ionomer series. As temperature increases, the relaxation time decreases as the thermally activated network gains mobility, and the supramolecular linkages become less effective. This trend is observed independently of the metal cations and the ionic content. The relaxation time increases with increasing ionic fraction. Comparison of the three series gives information about the role of the counter ion on the strength and dynamics of the ionic clusters. It is observed that the relaxation times are generally low ($\tau_b < 10$ s) for Na^+ based ionomers with an ion fraction of 6 % and lower. In the case of the Zn^{2+} and Co^{2+} based ionomers (Figures 3b and c), a similar trend is observed. The results indicate that already at low ion fractions, the most stable ionic bonds are formed in the Co^{2+} -based ionomers, followed by Zn^{2+} .

For the 8% and higher ionic content, the PNa series displays a remarkable deviation from the normal behavior i.e there is no crossover of G' and G'' . At 25 °C and 100 Hz, PNa-8 has a G' and G'' of 1.5 and 0.85 MPa, respectively. In these high Na^+ content samples, the G' stays greater than G'' for the entire frequency range of measurement, indicating that the crossover frequency ω_{cr} and the τ_b is beyond the measurement range (i.e. below 10^{-4} Hz). On the contrary, the PZn and PCo series, despite the higher valence of the involved counter ions (Zn^{2+} and Co^{2+}), show the typical dynamic crossover frequency above 10^{-4} Hz at room temperature, which further suggests the presence of different supramolecular interactions in higher Na^+ content ionomers. In comparison to the other two cations, the behavior of PNa series may be attributed to the higher chemical affinity of the monovalent Na^+ ion to the carboxylate acid groups resulting in larger clusters and thus result in a lower density of effective tie points in the ionomer network.

In order to obtain a better insight into the thermally activated flow of the materials below the thermal transition temperature of the ionic clusters (T_i), we perform an Arrhenius analysis by plotting τ_b logarithmically against the reciprocal temperature, and extracting the apparent activation energy (E_a) of the relaxation process.^{26, 39}

$$\tau_b = A_0 \cdot e^{\frac{E_a}{RT}} \quad (2)$$

As illustrated for the PNa, PZn and PCo series in Figure 4, the results of the Arrhenius analysis is consistent with the qualitative observations. For the PCo series, E_a is significantly higher than that for PZn and PNa with similar ionic contents, and follows the trend of $E_a(\text{PCo}) > E_a(\text{PZn}) > E_a(\text{PNa})$. All E_a values determined are in the range of 40-150 kJ mol^{-1} , and increase with increasing ionic fraction. Similar value for the apparent activation energy E_a ranging from 62 to 95 kJ mol^{-1} has been reported for ethylene-methacrylic acid ionomers neutralized with Na^+ .⁴⁰ Similar temperature dependences of activation energy for breakage of supramolecular bonds has been previously reported for other systems. Noro et al. observed an Arrhenius-type activation energy for breakage of hydrogen bonds between copolymer blocks of thermoplastic elastomers.⁴¹ Le et al. reported an Arrhenius-type temperature dependence of the viscosity with the activation energy which levels off at low fractions of the

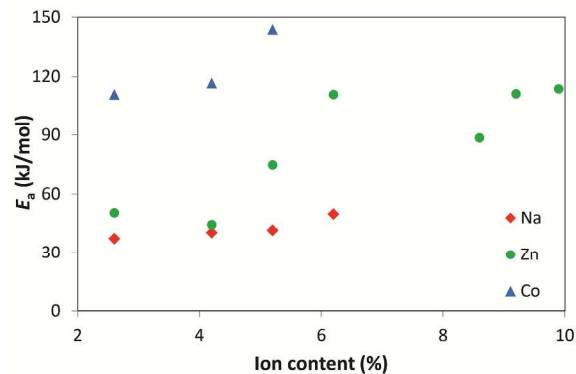


Fig 4. Relation between activation energy for different ionic contents for PNa, PZn and PCo series.

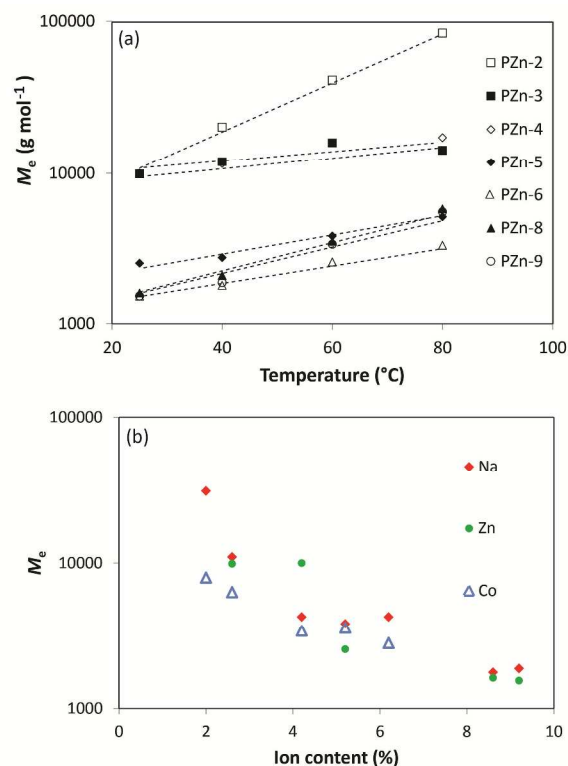


Fig 5. (a) M_e vs. temperature for PZn series and (b) comparison of M_e for different ionic content of PNa, PZn and PCo series at room temperature. Dotted lines are a guide to the eye.

hydrogen bonding moiety.⁴²

Effect of network mobility

The dynamic rheological frequency sweep tests show that for all the studied samples the ionic clusters act as effective crosslinks at short times (high frequencies), indicated by $G' > G''$. The materials act as effective elastomers characterized by a constant modulus over a range of frequencies, known as the rubbery plateau. The storage modulus in this plateau zone is called the plateau modulus (G_N) and is inversely proportional to the segment length M_e according to⁴³

$$G_N = \rho RT / M_e \quad (3)$$

where ρ is the measured density of the ionomers, 1 g cm^{-3} ;

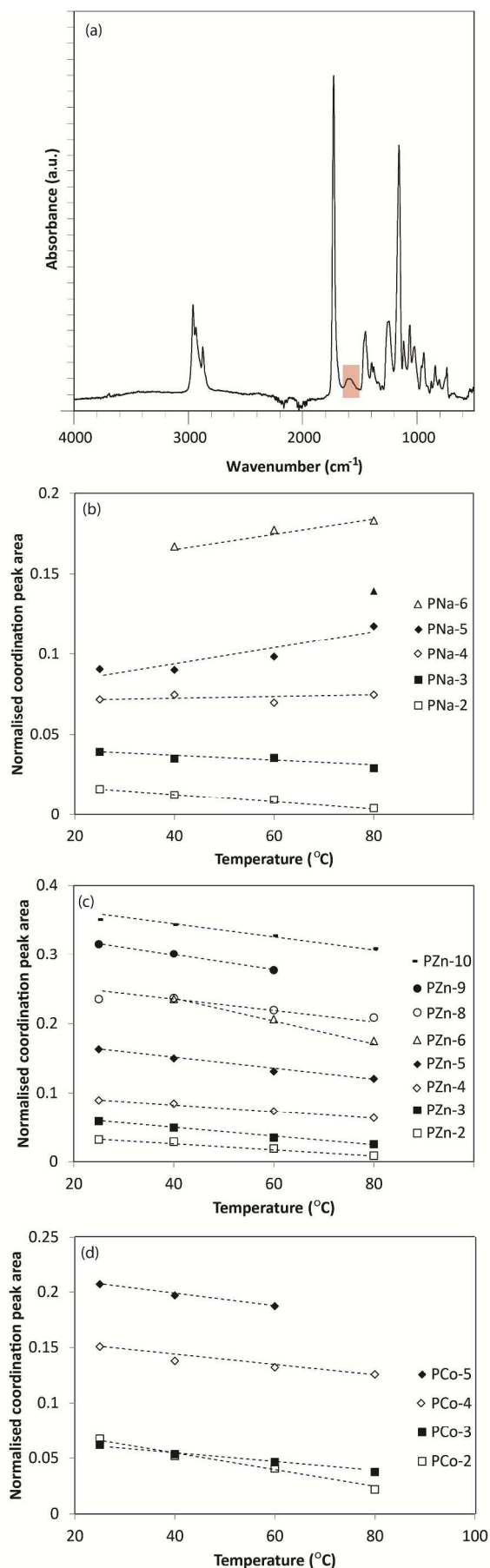


Fig 6. (a) Representative FTIR spectrum of PCo-6 with the shaded region showing of the coordination peak. Area of coordination peak normalized to the carbonyl stretch obtained via FTIR as a function of temperature for varying ionic content and different metal ions (b) Na⁺, (c) Zn²⁺ and (d) Co²⁺. Dotted lines are a guide to the eye.

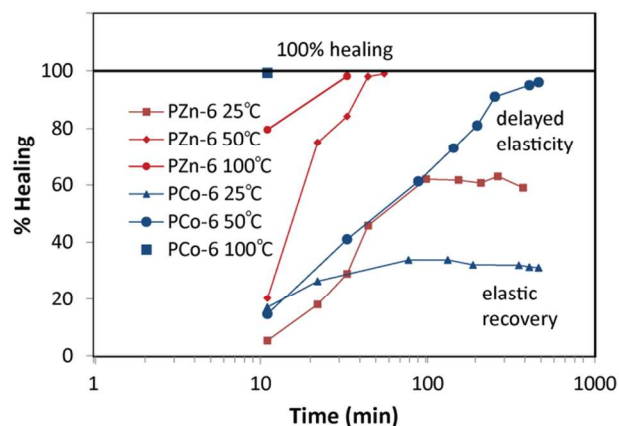


Fig 7. Time dependent scratch healing efficiency for PZn-6 and PCo-6 ionomers at different temperatures.

R is the universal gas constant, $8.314 \text{ J K}^{-1} \text{ mol}^{-1}$,
 T is the temperature of measurement and
 M_e is the apparent average molecular weight between crosslinks.

The relation is valid for model networks with covalent
 15 crosslinks, but can be applied as a relative measure also on more
 complex systems. In practice, the modulus of the plateau region
 shows the relative changes in the effective segment length M_e or
 the apparent crosslink density as compared to a standard material.
 In samples where a final plateau modulus was beyond the high
 20 frequency measurement range of the rheometer (i.e. 100 Hz), an
 extrapolated modulus value was used. A low M_e value indicates a
 network with a greater degree of crosslinks or tie points, and can
 be used to describe the mobility of the supramolecular network.<sup>29,
 44, 45</sup> M_e calculated from equation (3) is typically considered a net
 25 effect, measured as a result of all effective entanglements
 including the polymer chain entanglements as well as those
 resulting from the ionic clusters. For the pure PnBA polymer, the
 plateau modulus G_N is 0.11 MPa, thus resulting in an M_e of 22500
 g mol^{-1} , which is representative of the entanglements resulting
 30 from only the polymer backbone. Upon incremental addition of
 ionic interactions and clusters, M_e is expected to decrease. When
 the ionic interactions are weak, i.e. for samples with <2% ionic
 groups, the plateau modulus is close to that of the pure PnBA.
 The pure polymer and ionomers with <2% metal content behave
 35 as viscous gels, and flow at all temperatures used in this study.
 Thus, they are not suitable for studying thermally activated self-
 healing and hence have been excluded from this work. As
 exemplified in Figure 5a for the PZn series, the effective segment
 length M_e decreases with increasing ion fraction in all three
 40 ionomer series, in accordance with the development of a stronger
 supramolecular network.

A comparison of the different cations at room temperature is
 shown in Figure 5b. For PNa-2 the ionomer acts as a loosely
 bound network as suggested by the high values of M_e . On the
 45 contrary PCo-2 has significantly low M_e , indicating more

Cite this: DOI: 10.1039/c0xx00000x

www.rsc.org/xxxxxx

ARTICLE TYPE

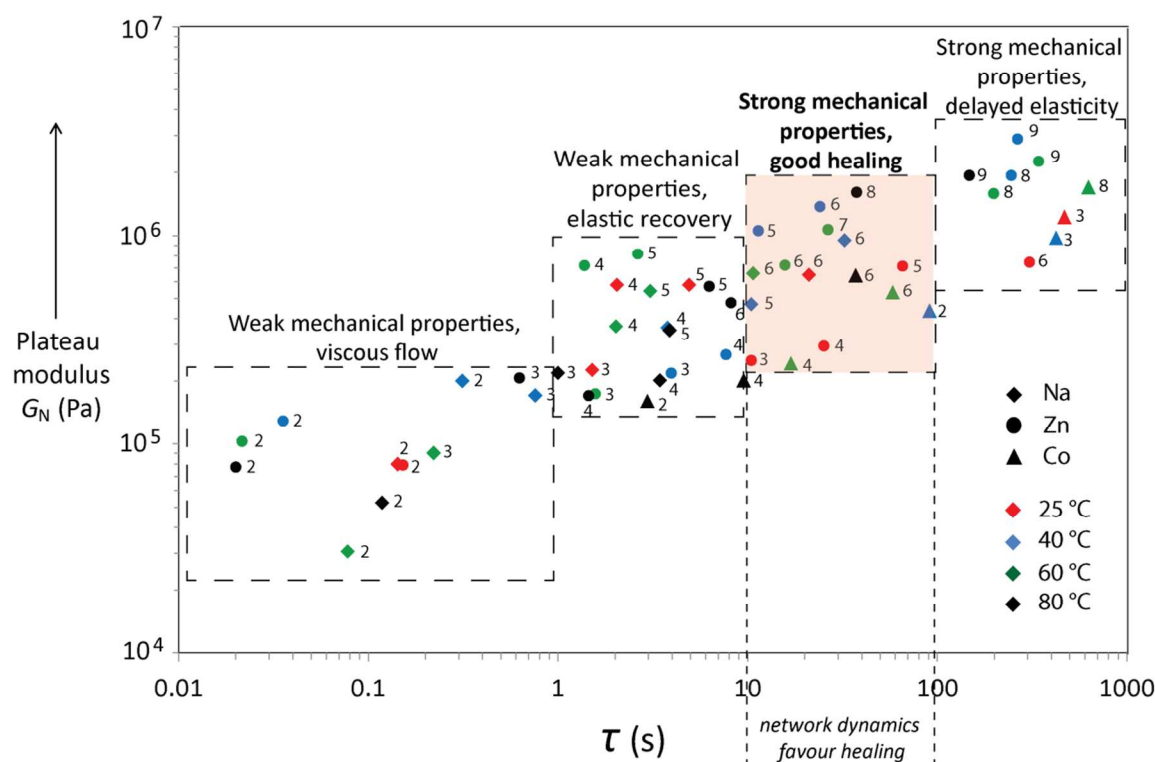


Fig 8. Correlation of rheological behavior to the macroscopic scratch healing data. Each series is represented by a symbol, and the filled color represents the temperature of measurement.

crosslink points. In the case of PNa series, remarkable drops in M_e are observed when comparing PNa-3 to PNa-2 and also comparing PNa-4 to PNa-3. The critical molecular weight for entanglement of linear poly(butyl acrylate) has been reported as $\sim 25000 \text{ g mol}^{-1}$,^{46, 47} which is lower than the M_n of these ionomers. For the Over the studied range of temperatures, the ionic clusters gain mobility which is represented in the increase in M_e . However, complete disintegration of the clusters does not occur for the high metal contents, as shown by M_e values ranging from ~ 4000 to 8000 g mol^{-1} . For the high metal content, 8% and greater, M_e ranges from ~ 800 to 1800 g mol^{-1} at room temperature and ~ 1800 to 5000 g mol^{-1} at $80 \text{ }^\circ\text{C}$. The M_e data for the PNa series and the PZn series show similar trends. This is in agreement with the absence of crossover frequency observed for the high Na content ionomers. Since Na is a stronger cation, it most likely forms bigger clusters with the highest number of ionic multiplets per cluster. This results in a low cluster density, albeit with very strong physical tie points and thus exhibit a high M_e . On the other hand Zn^{2+} and Co^{2+} are larger cations with delocalized charges and thus form smaller clusters. They most likely have higher density of clusters, resulting in more physically crosslinked networks and thus with lower M_e . Moreover, Co^{2+} , is more electropositive and has a greater delocalization of charge, resulting in the most physically crosslinked network compared to

Na^+ and Zn^{2+} , which is also apparent in the higher E_a of dissociation of ionic clusters, shown in Figure 4. Similar aggregation behavior has been observed for monofunctional and bifunctional supramolecular polymers.^{15, 24, 48}

Cluster formation

Temperature dependent FTIR analysis was used to obtain information regarding the extent of dissociation of metal-carboxylate bonds. A representative FTIR spectrum is shown in Figure 6(a) and the coordination peak from 1660 to 1512 cm^{-1} wavenumber used for quantification is highlighted. The ratios of the peak area of the coordination peak to the carbonyl stretch are plotted against temperature for the PNa, PZn and PCo series in Figure 6(b), (c) and (d), respectively. With the exception of PNa series, the relative intensity of the metal carboxylate peak decreases with increasing temperature as the ionic clusters gain greater mobility. The degree of coordination is similar for the 2 and 3% ion content samples but increases more rapidly with the 4% and higher samples. This is corroborated by the E_a and G_N data. Remarkably, in the case of the PNa series, the extent of metal coordination increases with the temperature for the 5% and higher samples. This is indicative of a higher degree of clustering with temperature. Upon thermal activation, the network gains mobility and recombination of Na^+ and COO^- groups is induced

resulting in more clusters. Due to its monodentate nature, Na⁺ easily forms weak physical tie points at room temperature, which restrict the network mobility as evidenced by τ_b and M_e trends. However, upon increasing the temperature, the polymer chains become more mobile and subsequently form a higher degree of supramolecular clustering. This is in good agreement with the rheology data which shows a permanently crosslinked network for the higher Na⁺ content ionomers even at higher temperatures.

Surface scratch healing

The surface scratch healing efficiencies for representative ionomers PZn-6 and PCo-6 are shown in Figure 7. At room temperature, both ionomers are unable to heal the damage and healing efficiency plateaus at 60 and 31%. This is most likely due to a recovery that is predominantly elastic in nature. The PCo-6 has slower rate of scratch healing which can be attributed to a higher degree of chain entanglement, which reduces polymer chain mobility. At 50 °C, both ionomers show sufficient chain mobility, and 100% scratch healing efficiency was observed. However, the rate of healing is slow, indicating that a thermally induced delayed elasticity contributes to the recovery.⁴⁹ Delayed elasticity refers to the intermediate range of temperatures where the viscoelastic polymer behavior is in between that of perfectly elastic solids and viscous liquids.⁵⁰ At 100 °C, PZn-6 and PCo-6 showed complete recovery at 33 and 11 minutes, respectively. As shown in Figure 1, healing occurs when the ion pairs undergo clustering to form a hierarchical network structure. Upon heating after any macroscopic damage such as a scratch, the polymer network rearranges to form ion pairs, further resulting in ionic multiplets and clusters which are regions of restricted mobility. Thus formation of this hierarchical network structure restores the original mechanical strength of the network. The scratch healing results are in agreement with the rheological measurements and thus the time and temperature conditions for healing of macroscale damage can be predicted by observing the chain dynamics of these polymers.

Relation between network mobility and healing

In order to obtain a correlation between network mobility given by reversible clusters and macroscale flow leading to healing, the plateau modulus as determined from the rheological data was plotted against the relaxation time τ_b of the ionomers in Figure 8. We obtain a master plot indicating a direct relationship between the two characteristic values on a double-logarithmic scale. A plateau modulus is developed only for materials with τ_b of 10⁻² s and longer. Ionomers with $\tau_b > 100$ s develop strong and permanent elastic properties. Taking into account the scratch healing data, the materials at different temperatures can further be classified in four different categories that correlate with their location in the master plot as indicated by the boxes (Figure 8). For $\tau_b < 10$ s, the ionomer is characterized by weak mechanical properties at the respective temperature, with either viscous flow or elastic recovery upon scratching. On the other extreme, if $\tau_b > 100$ s, the ionomers show strong mechanical properties and reach only partial scratch healing due to restricted network mobility. Finally, in the intermediate range of τ_b , i.e. 10 s < τ_b < 100 s we find ionomers showing good scratch healing behavior and good mechanical properties as highlighted in Figure 8. This time regime is partly in agreement with earlier reports, where a

dynamic bond lifetime of $1 \mu\text{s} < \tau_b < 60$ s is suggested.²⁴ While the latter is a parameter of the single bond, the network integrity of ionomers is characterized by multiple involvement of a polymer chain in several multiplets acting as multifunctional network points, and thus the relaxation time in such networks is supposed to be longer than that for the individual bond. In addition to a critical range of time scale of 10 s < τ_b < 100 s, the master plot delivers the plateau modulus as an additional important parameter for efficiently self-healing materials. Moreover, the results show that scratch tests combined with network dynamics tests enabled a correlation between macroscopic damage recovery and supramolecular reversibility of these ionomers.

Conclusions

Model ionomers based on poly(butyl acrylate-co-acrylic acid) with varying fraction of ionic groups and the respective Na⁺, Zn²⁺ and Co²⁺ counter ions were used to investigate the role of reversible interactions and network mobility on healing. Upon increasing the ionic content, there is a significant increase in cluster formation and a stronger temperature dependence, while still exhibiting reversibility. The degree of network reversibility as predicted by rheology and calculated as the activation energy of cluster dissociation can be correlated to macroscale scratch healing. Ionomers with 10 s < τ_b < 100 s have a good network reversibility which yields fast and complete scratch healing and have good mechanical properties. Further research on other supramolecular systems is needed to ascertain if similar critical ranges of τ_b can be established, which can predict a good balance between network mobility and reversible interactions resulting in completely self-healing dynamic networks.

Notes and references

- ^a *Novel Aerospace Materials, Faculty of Aerospace Engineering, Delft University of Technology, Kluyverweg 1, Delft 2629HS, The Netherlands;* *E-mail: s.j.garciaespallargas@tudelft.nl
^b *Chemistry Department, University of Cologne, D-50939 Cologne, Germany;* †E-mail: annette.schmidt@uni-koeln.de
1. Y. C. Yuan, T. Yin, M. Z. Rong and M. Q. Zhang, *Express Polymer Letters*, 2008, **2**, 238-250.
 2. S. van Der Zwaag, in *Self Healing Materials – an Alternative Approach to 20 Centuries Materials Science* ed. S. van der Zwaag, Springer, Dordrecht, The Netherlands, 2007.
 3. B. Jamil, P. Heidi and S. Amit, in *Smart Coatings III*, American Chemical Society, 2010, vol. 1050, pp. 3-20.
 4. A. P. Esser-Kahn, N. R. Sottos, S. R. White and J. S. Moore, *Journal of the American Chemical Society*, 2010, **132**, 10266-10268.
 5. X. Chen, M. A. Dam, K. Ono, A. Mal, H. Shen, S. R. Nutt, K. Sheran and F. Wudl, *Science*, 2002, **295**, 1698-1702.
 6. Y. Zhang, A. A. Broekhuis and F. Picchioni, *Macromolecules*, 2009, **42**, 1906-1912.
 7. J.-M. Lehn, *Progress in Polymer Science*, 2005, **30**, 814-831.
 8. J. Canadell, H. Goossens and B. Klumperman, *Macromolecules*, 2011, **44**, 2536-2541.
 9. P. Zheng and T. J. McCarthy, *Journal of the American Chemical Society*, 2012, **134**, 2024-2027.
 10. L. M. Meng, Y. C. Yuan, M. Z. Rong and M. Q. Zhang, *Journal of Materials Chemistry*, 2010, **20**, 6030-6038.

11. N. Holten-Andersen, M. J. Harrington, H. Birkedal, B. P. Lee, P. B. Messersmith, K. Y. C. Lee and J. H. Waite, *Proceedings of the National Academy of Sciences*, 2011, **108**, 2651-2655.
12. G. R. Whittell, M. D. Hager, U. S. Schubert and I. Manners, *Nat Mater*, 2011, **10**, 176-188.
13. J. Yuan, X. Fang, L. Zhang, G. Hong, Y. Lin, Q. Zheng, Y. Xu, Y. Ruan, W. Weng, H. Xia and G. Chen, *Journal of Materials Chemistry*, 2012, **22**, 11515-11522.
14. P. Cordier, F. Tournilhac, C. Soulie-Ziakovic and L. Leibler, *Nature*, 2008, **451**, 977-980.
15. F. Herbst, K. Schröter, I. Gunkel, S. Gröger, T. Thurn-Albrecht, J. Balbach and W. H. Binder, *Macromolecules*, 2010, **43**, 10006-10016.
16. R. Maoz, J. Sagiv, D. Degenhardt, H. Möhwald and P. Quint, *Supramolecular Science*, 1995, **2**, 9-24.
17. S. J. Kalista and T. C. Ward, *Journal of The Royal Society Interface*, 2007, **4**, 405-411.
18. R. J. Varley and S. van der Zwaag, *Acta Materialia*, 2008, **56**, 5737-5750.
19. M. J. Serpe and S. L. Craig, *Langmuir*, 2006, **23**, 1626-1634.
20. F. Herbst, S. Seiffert and W. H. Binder, *Polymer Chemistry*, 2012, **3**, 3084-3092.
21. S. Hackelbusch, T. Rossow, P. van Assenbergh and S. Seiffert, *Macromolecules*, 2013, **46**, 6273-6286.
22. D. Xu, C.-Y. Liu and S. L. Craig, *Macromolecules*, 2011, **44**, 2343-2353.
23. W. C. Yount, D. M. Loveless and S. L. Craig, *Angewandte Chemie International Edition*, 2005, **44**, 2746-2748.
24. T. Aida, E. W. Meijer and S. I. Stupp, *Science*, 2012, **335**, 813-817.
25. A. M. Grande, L. Castelnovo, L. D. Landro, C. Giacomuzzo, A. Francesconi and M. A. Rahman, *Journal of Applied Polymer Science*, 2013, **130**, 1949-1958.
26. B. Hird and A. Eisenberg, *Journal of Polymer Science Part B: Polymer Physics*, 1990, **28**, 1665-1675.
27. F. Herbst and W. H. Binder, in *Self-Healing Polymers*, Wiley-VCH Verlag GmbH & Co. KGaA, 2013, pp. 273-300.
28. S. J. Garcia, *European Polymer Journal*, 2014, **53**, 118-125.
29. F. Herbst, S. Seiffert and W. H. Binder, *Polymer Chemistry*, 2012.
30. S. Seiffert and J. Sprakel, *Chemical Society Reviews*, 2012, **41**, 909-930.
31. R. A. Weiss, A. Sen, C. L. Willis and L. A. Pottick, *Polymer*, 1991, **32**, 1867-1874.
32. S. Kutsumizu, H. Hara, H. Tachino, K. Shimabayashi and S. Yano, *Macromolecules*, 1999, **32**, 6340-6347.
33. R. K. Shah and D. R. Paul, *Macromolecules*, 2006, **39**, 3327-3336.
34. N. Hohlbein, A. Shaaban, A. R. Bras, W. Pyckhout-Hintzen and A. M. Schmidt, *submitted*, 2014.
35. K. Han and H. L. Williams, *Journal of Applied Polymer Science*, 1991, **42**, 1845-1859.
36. J. M. Vega, A. M. Grande, S. van der Zwaag and S. J. Garcia, *European Polymer Journal*, 2014, **57**, 121-126.
37. F. Herbst, D. Döhler, P. Michael and W. H. Binder, *Macromolecular Rapid Communications*, 2013, **34**, 203-220.
38. E. B. Stukalin, L.-H. Cai, N. A. Kumar, L. Leibler and M. Rubinstein, *Macromolecules*, 2013, **46**, 7525-7541.
39. G. Tsagaropoulos and A. Eisenburg, *Macromolecules*, 1995, **28**, 396-398.
40. N. K. Tierney and R. A. Register, *Macromolecules*, 2002, **35**, 6284-6290.
41. A. Noro, Y. Matsushita and T. P. Lodge, *Macromolecules*, 2008, **41**, 5839-5844.
42. J. Li, J. A. Viveros, M. H. Wrue and M. Anthamatten, *Advanced Materials*, 2007, **19**, 2851-2855.
43. C. M. Roland, in *Viscoelastic Behavior of Rubbery Materials*, Oxford University Press, 2011.
44. K. Hackethal, F. Herbst and W. H. Binder, *Journal of Polymer Science Part A: Polymer Chemistry*, 2012, **50**, 4494-4506.
45. K. E. Feldman, M. J. Kade, E. W. Meijer, C. J. Hawker and E. J. Kramer, *Macromolecules*, 2009, **42**, 9072-9081.
46. A. Zosel and G. Ley, *Macromolecules*, 1993, **26**, 2222-2227.
47. C. Former, J. Castro, C. M. Fellows, R. I. Tanner and R. G. Gilbert, *Journal of Polymer Science Part A: Polymer Chemistry*, 2002, **40**, 3335-3349.
48. B. Ghosh, K. V. Chellappan and M. W. Urban, *Journal of Materials Chemistry*, 2012, **22**, 16104-16113.
49. S. J. Garcia, H. R. Fischer and S. van der Zwaag, *Progress in Organic Coatings*, 2011, **72**, 211-221.
50. I. L. Hopkins and C. R. Kurkjian, in *Physical Acoustics V2B: Principles and Methods*, ed. W. P. Mason, Academic Press, 2012.